BNL-64071
Informal Report

ADVANCED ZINC PHOSPHATE CONVERSION COATINGS

Phase II

Final Report
(June 1996-December 1996)

by

C.I. Handsy and T. Sugama*

ATSTA-TMC
U.S. Tank Automotive Command
Warren, MI 48090-9055

* Department of Applied Science
Brookhaven National Laboratory
Associated Universities, INC.
Upton, Long Island, NY 11973

This work was performed under the auspices of the U.S. Department of Energy, Washington, D.C. under Contract No. DE-AC02-76CH00016, and supported by the U.S. Tank Automotive Command, under Contract MIPR-EH62Y739.

DISCLAIMER

ABSTRACT

A SERDP-sponsored program aims at developing environmentally benign zinc phosphate conversion coatings and their process technologies for the electrogalvanized steel (EGS). we succeeded in formulating an environmentally acceptable phosphate solution without Co- and Ni-related additives, and also in replacing a hexavalent Cr acid sealant applied over the zinc phosphate (Zh·Ph) layers with a water-based polysiloxane sealers. The specific advantages of the newly developed Zn·Ph coatings were as follows: 1) there was rapid growth of uniform, dense embryonic Zn·Ph crystals on the EGS surfaces due to the creation of short-circuited cells with Mn acting as the cathode and the galvanized (zinc) coatings as the anode, 2) an excellent protection layer against corrosion was formed, extending the service life of zinc layers as galvanic sacrifice barriers, and 3) adhesion to the electro-deposited polymeric primer coating was improved because of the interaction between the siloxane sealer and primer. A full-scale demonstration to evaluate the reproducibility of this new coating technology on mini-sized automotive door panels made from EGS was carried out in collaboration with the Palnut Company (as industrial coating applicator) in New Jersey. All of the 150 mini-door panels were successfully coated with Zn·Ph.

1. Introduction

In the previous SERDP-sponsored program aimed at developing environmentally benign zinc phosphate conversion coatings and their process technologies for cold-rolled steel (CRS) substrates [1], we succeeded in formulating an environmentally acceptable phosphating solution without Co- and Ni-related additives. The basic formulation consisted of 5 wt% $Zn_3(PO_4)_2 \cdot 2H_2O$, 10 wt% (86 % H_3PO_4), 3 wt% poly(acrylic acid) [p(AA)] and 82 wt% water; appropriate amounts of the $Mn(NO_3)_2 \cdot 6H_2O$ and $FeSO_4 \cdot 7H_2O$ as additives were incorporated into this basic formulation. These additives had two important functions; one was to create a large number of nucleated sites of embryonic Zn·Ph crystals on the steel surfaces, and the other was to act as an inhibitor of corrosion. The p(AA)-modified Zn·Ph coatings not only displayed an excellent salt-spray resistance of > 1000 hrs, but also showed a strong electrochemical affinity with the electro-deposited polymeric primer coatings.

In the automotive industry, it is commonly known that electroplated coatings of pure zinc and various zinc alloys over steel surfaces are responsible for improving corrosion resistance by delaying the onset of "red rust" of body panels and various discrete parts, such as fasteners and brackets [2]. Pure zinc coatings currently have the major share of the automotive body-panel market. Although the art of making electroplated zinc coating for electrogalvanized coatings is well developed, two problem areas still remain. One problem is the poor adherent property of galvanized (Zn) coating surfaces to the polymeric topcoats, and the other is the necessity of post-treatment to inhibit the onset of "white rust", which represents deterioration of the zinc layer. The former problem relating to the paint's adhesion properties is due primarily to the chemically inert, smooth texture of coating surfaces. One method to solve this problem is to increase the roughness of the surface either by etching or by sandblasting [3]. Such roughening procedures, which increase the actual surface area, provide more mechanical interlocking bonds at interfaces between the paint and the Zn coating. However, there is no resolution to inhibiting the onset of "white rust" of Zn coatings. Thus, modifying the zinc coating surfaces is essential to improve their chemical and physical affinities for the primers, and to retard the corrosion themselves.

Based upon the information described above, our executive plan for FY 1996 was placed on three major topics: the first was to evaluate the phosphating

solutions and process technologies developed in the previous year, and if necessary, to reformulate their basic chemical composition for the electrogalvanized steel (EGS) surfaces; the second focus was on developing water-based sealants for replacing a Cr acid sealant used commonly as a sealing agent of Zn·Ph coating layers; and third, to apply any new phosphating technology emerging from these two areas to mini-sized automobile door panels made from EGS in the pilot plant at Palnut Company in New Jersey. The first topic included exploring the morphological features, identifying the phases and surface chemical state of the p(AA)-modified Zn·Ph coating layers deposited onto the EGS surfaces, as well as investigating their ability to protect the zinc layers in the EGS against white rust-related corrosion. Under the second topic, our attention was paid to surveying the characteristics of water-based sealants which improve the effectiveness of Zn·Ph coatings in preventing the corrosion of EGS, and also have a great affinity for the electro-deposited polymeric primers. All the data obtained were correlated directly with the results from a full-scale feasibility test to demonstrate the reproducibility of this new coating technology.

2. Experimental Details

2.1 Materials

The metal substrate used was ASE 1006 cold-rolled steel coated with electroplated zinc (EGS, Ford E 60 Electrozinc 60G), supplied by Advanced Coating Technologies, Inc.. The formulation for the basic zinc-phosphate liquid was 5.0 wt% zinc orthophosphate dihydrate (Alfa Co.), 10.0 wt% H_3PO_4, 1.0 wt% $Mn(NO_3)_2 \cdot 6H_2O$ (Alfa Co.) and 84.0 wt% water. In modifying this standard formulation, a 25 % p(AA) colloidal solution (Rohm and Hass, Co.) added to the standard phosphating solution was 3.0 wt% of the total standard solution. The average molecular weight of the p(AA) was 60,000. As a water-based polysiloxane sealant, 3-aminopropyltrimethoxy-silane (APS) monomer, was supplied by Petrarch Systems Ltd.. The APS precursor sealant consisted of a 7 wt% APS, 3 wt% methylalcohol, 0.7 wt% hydrochloric acid and 89.3 wt% water, and had a pH of 9.96. The APS-sealed Zn·Ph coatings on the EGS test panels were prepared in according with the following sequence: As a first step to remove surface contaminants, the EGS panels were dipped for 1 min at 25°C into a pickling solution consisting of 2 wt% phosphoric acid, 1 wt% sulfonic acid, and 97 wt% water. The pickle-cleaned EGS panels were then immersed into the p(AA)-modified zinc phosphate make-up solution

for ≈ 1 min at 80°C, withdrawn slowly, followed by rinsing them with water to wash off any acid contaminants from the Zn·Ph surfaces. Next, the rinsed Zn·Ph panels were dipped for few seconds into the APS precursor sealant. Finally, the APS-wetted Zn·Ph panels were dried for 30 min in an oven at temperature of 150°C to form the polymeric APS sealant over the Zn·Ph surfaces, and to fill any voids and fissure spaces in the Zn·Ph layers.

In preparing the polymeric primer coating, all the APS-sealed Zn·Ph panels were coated with the polyurethane-modified epoxy copolymer (POWERCRON 648) by electrodeposition technology at Advanced Coating Technologies, Inc. The polymeric primer was cured in an oven at ≈ 177°C for 30 min.

2.2 Measurements

Scanning electron microscopy (SEM) was used to investigate the degree of coverage of the EGS surfaces by p(AA)-modified Zn·Ph coatings and explore the alteration in morphological feature of crystalline Zn·Ph coatings as a function of immersion time. The surface chemical states and phase identification of the coating were carried out using x-ray photoelectron spectroscopy (XPS) and x- ray diffraction (XRD). The concentration of zinc ions dissociated from the EGS surfaces in single H_3PO_4 and $Mn(NO_3)_2 \cdot 6H_2O$ aqueous solutions, and in their combined medium was determined by atomic absorption spectrophotometry (AA).

DC potentiodynamic polarization measurement for data on the rate of corrosion was made with an EG&G Princeton Applied Research Model 362-1 Corrosion Measurement System. The electrolyte was a 0.5 N sodium chloride solution, made from distilled water and reagent grade salt. The test panel was mounted in a holder, and then inserted into a EG&G Model K47 electrochemical cell. The tests were conducted in an aerated 0.5 M NaCl solution at 25°C, on an exposed surface area of 1.0 cm^2. The polarization curves containing the cathodic and anodic regions were measured at a scan rate of 0.5 mv/sec in the corrosion potential range of -1.1 to -0.3 volts. AC electrochemical impedance spectroscopy (EIS) was used to evaluate the ability of coating films to protect the EGS from corrosion. The test panel was mounted in a holder, and then inserted into an electrochemical cell. Computer programs were established to calculate theoretical impedance spectra and to analyze the experimental data. Specimens with a surface area of 13 cm^2 were exposed to an aerated 0.5 N NaCl electrolyte at 25°C, and single-sine technology with an input AC voltage of 10 mV (rms) was used over a frequency

range of 10 KHz to 2 mHz. The lower frequency limit was chosen because of time limitations. To estimate the protective performance of coatings, the impedance, $|Z|$ ohm-cm^2, was determined from the plateau in Bode-plot scans that occurred at low frequency regions. The 5% salt-spray tests at 35°C for the unprimed Zn·Ph coating panels were conducted to evaluate the degree of white rusting on unscribed panel surfaces. The salt-spray tests for the primed Zn·Ph coating panels were carried out in accordance with ASTM D 1654-79a, evaluating the blistering associated with corrosion and the loss of adhesion of the primer coating at a scribe mark, or other failure of primer film.

3. Results and Discussion

3.1 p(AA)-Modified Zn·Ph Coatings on EGS

Figure 1 shows SEM micrographs of crystalline Zn·Ph coatings derived from the p(AA)-modified phosphating solutions as a function of the immersion time of the EGS substrate into the phosphating bath at 80°C. As is seen, the growth of lamellar-like crystals was observed after immersion for only 2 sec (b), compared with the surface texture of the 1 sec-treated EGS (a). Immersion for 5 sec was sufficient to produce dense conversion coatings over the entire substrate surface (see Fig. 1-c). A further extension of immersing time to 10 sec (d) revealed a densely packed conformation of lamellar Zn·Ph crystals, reflecting that the EGS surface had essentially been altered and now had a rough microstructure.

Figures 2 and 3 show the high-resolution XPS spectra of P_{2p}, $Zn_{2p3/2}$, and C_{1s} core-level excitations for the Zn·Ph coatings as a function of treatment time. In the P_{2p} region (Fig. 2), no peak was found on the "as-received" EGS surfaces denoted as "OS". The coating made by 1 sec dipping (1S) exhibited two weak peaks, at 133.9 and 132.4 eV. The former peak presumably reveals the P originating from the Zn·Ph [4], and the latter may be due to the formation of zinc dihydrogen orthophosphate, $Zn(H_2PO_4)_2 \cdot xH_2O$ salt [5]. The intensity of peak at 133.9 eV markedly increased with an increased treatment time, while the peak at 132.4 eV vanished. The degree of coverage of Zn·Ph over EGS can be confirmed by comparing the spectral features of the $Zn_{2p3/2}$ region (Fig. 3). The single peak at the BE position of 1022.2 eV for the "as-received" EGS (OS) is due to Zn in the ZnO layers [6,7], forming on the top surface of galvanized coatings. The $Zn_{2p3/2}$ curve of the 2 sec-treated specimens (2S) is distinctive; an additional weak line at 1023.0 eV appears in the spectrum, separate from the main line. The intensity of

this new line dramatically increased as the treatment time was prolonged. After 5 sec (5S), this peak eventually became the principal line, while the line at 1022.2 eV, originating from the Zn in ZnO, disappeared. Because, the peak at 1023.0 eV belongs to Zn originating from Zn·Ph [8], this result strongly supported the SEM data showing that an immersion of 5 sec is long enough to cover the whole surface of EGS with Zn·Ph. The C_{1s} region of the untreated EGS surfaces (Fig.3-0S) had a symmetrical peak at 285.0 eV, reflecting the C in the hydrocarbon, "CH_n", contaminant. When this EGS surface was treated with a phosphating solution for 2 sec, the C_{1s} spectrum (2S) revealed that the two resolvable Gaussian components at 285.0 eV as the principal component is not only attributable to hydrocarbon in the organic contaminant, but also to that in the backbone chain of p(AA). A second peak emerging at 288.7 eV corresponds to carbon originating from the carboxylic acid, COOH, in the P(AA) [9]. Increasing the treatment time to 10 sec showed the emergence of an additional peak at 287.2 eV in the spectrum (10S). We assigned this additional peak, emerging at the BE location between a carbonyl carbon, C=O, at ≈ 288.0 eV and a carbon-oxygen single bond at ≈ 286.5 eV [10], to the C in the $-COO^{-}-Zn^{2+}-^{-}OOC-$ salt complex formation [11, 12]. Nevertheless, both the bulk and complexed p(AA) polymers appear to be present at the outermost surface site of Zn·Ph.

An important question remains to be solved: namely, why the $Mn(NO_3)_2 \cdot 6H_2O$-incorporated solution causes the rapid deposition of Zn·Ph on the EGS surfaces. To investigate the electrochemical activity of the $Mn(NO_3)_2 \cdot 6H_2O$ reagent in the increase in the conversion rate of Zn·Ph, we used three solutions without the $Zn_3(PO_4)_2 \cdot 2H_2O$ and p(AA) reagents; 1) 10.0 wt% H_3PO_4-90.0 wt% water, 2) 1.2 wt% $Mn(NO_3)_2 \cdot 6H_2O$-98.8 wt% water, and 3) 10.0 wt% H_3PO_4-1.2 wt% $Mn(NO_3)_2 \cdot 6H_2O$-88.8 wt% water. The experimental work was performed in accordance with the following sequence. First, an EGS test panel with a surface area of 100 cm^2 was immersed for 2, 5, 10, or 30 sec, into a bath containing 1L of these solutions at 80°C. After withdrawing the panel, the concentration of Zn ion in the bath was detected by A.A. to gain the information on the anodic dissolution of the Zn coating. Figure 4 shows the resulting dissolution rates, μg/ml, of Zn ion from the Zn coating, as a function of immersion times. When the EGS panels were soaked in the single $Mn(NO_3)_2 \cdot 6H_2O$ solution, ≈ 2.7×10^{-4} μg/ml of Zn ions dissociate from the EGS surfaces in the first 2 sec of immersion; thereafter, the rate of Zn ion dissolution increases with increased time. The concentration of dissociated Zn

ion after 30-sec immersion was ≈ 1.8 x 10^{-3} μg/ml. Using the other single H_3PO_4 solution, the amount of Zn dissociated in 2 to 30 sec corresponded to a tenfold increase over that of the $Mn(NO_3)_2 \cdot 6H_2O$ solution. By comparison, a considerable amount of Zn ion was recorded from the combined solution of $Mn(NO_3)_2 \cdot 6H_2O$ and H_3PO_4; immersion for only 2 sec resulted in the dissociation of abundant Zn ion of near 2 x 10^{-1} μg/ml, and subsequently an increase in immersion to 30 sec referred to the dissolution of 1.1 μg/ml. In addition, the extent of hydrogen evolution which was observed by the bubbling of the phosphating solution surrounding the EGS panel was in the following order; H_3PO_4 + $Mn(NO_3)_2 \cdot 6H_2O$ >> H_3PO_4 >$Mn(NO_3)_2 \cdot 6H_2O$ solutions. These findings verified that the addition of $Mn(NO_3)_2 \cdot 6H_2O$ to H_3PO_4 solution significantly promotes the dissolution of Zn ions from the EGS surfaces in conjunction with a more brisk evolution of hydrogen. Possible interpretation of the electrolytic corrosion of Zn layers in the H_3PO_4 electrolyte containing Mn^{2+} ions is as follows: the electrochemical reaction between Zn and H_3PO_4 leads to the anodic dissolution of Zn, $Zn \rightarrow Zn^{2+} + 2e^-$, which is directly related to the corrosion of galvanized coatings. After the ejection of Zn ions, the electrons $2e^-$ generated by the anodic reaction of Zn preferentially react with the Mn^{2+} ions dissociated from the $Mn(NO_3)_2 \cdot 6H_2O$ reagents. This reaction can be described as the electron-trapping reaction, $Mn^{2+} + 2e^- \rightarrow Mn^\circ$ [13]. The elemental Mn which is less electropositive than Zn may adhere to the Zn to create short-circuited cells with Zn acting as the anodic area and Mn as the cathode. Assuming that the creation of such a short-circuited cell is reasonable, the reaction of Zn with H_3PO_4 might be accelerated by the presence of a cathodic Mn electrode. Once the dissolution of Zn ions has occurred at anodic area, the electrons pass from Zn to Mn, and then the uptake of electrons by hydrogen ions discharged from H_3PO_4 results in a brisker evolution of hydrogen from cathodic Mn side:

$$2H_3PO_4 \rightarrow 2H^+ + 2H_2PO_4^-$$

$$2H^+ + 2e^- \rightarrow H_2.$$

From this information, we show the hypothetic conversion mechanisms of Mn-incorporated H_3PO_4 solution into zinc phosphate phase over the EGS (Fig. 5). The anodically dissolved Zn^{2+} ions react with an ionic dihydrogen phosphate, $H_2PO_4^-$, formed by the discharge of H^+ from H_3PO_4 electrolyte. This reaction leads to the formation of zinc dihydrogen orthophosphate, $Zn(H_2PO_4)_2$, and subsequently, the hydration of $Zn(H_2PO_4)_2$ aids in its conversion into $Zn_3(PO_4)_3 \cdot nH_2O$. A similar

mechanism may occur when Mn-incorporated zinc phosphating solution was applied as a Zn·Ph-convertible solution. The only difference was that many free Zn ions, dissociated from $Zn_3(PO_4)_2 \cdot 2H_2O$ as the starting material, are present in the original phosphating bath before immersing the EGS plates. Thus, the anodic dissolution of Zn not only contributes to the precipitation of $Zn_3(PO_4)_2 \cdot nH_2O$ on the EGS, but also may have catalytical activity which increasingly promotes the rate of conversion of free Zn ions into the Zn·Ph.

Figure 6 illustrates the XRD tracing, ranging from 0.444 to 0.225 nm, of the "as-received" EGS as a control, and the p(AA)-modified Zn·Ph coatings prepared by immersing EGS panels for 1, 2, 5, and 10 sec. The XRD pattern of the control shows the presence of a single phase only corresponding to the pure Zn crystal. Although the intensity of XRD line is very weak, the Zn·Ph conversion products formed on EGS after immersing for 1 sec can be identified as the hopeite phase, $Zn_3(PO_4)_2 \cdot 4H_2O$. The intensity of these hopeite lines markedly increased with an increased immersion time, while the strong lines of the underlying Zn phase are still present in the pattern. The data also indicated that zinc orthophosphate dihydrate, $Zn_3(PO_4)_2 \cdot 2H_2O$ coexists as minor phase with the hopeite.

3.3 Water-Based APS Sealant

One drawback of the Zn·Ph coatings is the fact that some interstitial voids remain in the coating layers, so that the panels corrode in a short-term exposure to a corrosion environment. Although uniform, dense, continuous Zn·Ph coating layers were fabricated on the panels, there is a need to fill their void spaces with sealers. The goal of this part of the research was to gain technical information on the non-toxic, water-based APS sealant used to replace the conventional toxic hexavalent chromic acid as corrosion-inhibiting sealant. This involved investigating the effectiveness of APS sealer on improving the ability of Zn·Ph coating layers to prevent the corrosion of EGS panels, and also assessing the importance of the chemical affinity of APS for the electro-deposited polymeric primer in extending salt-spray resistance.

In the XPS study earlier, we found that the p(AA) polymers remain at the outermost surface sites of Zn·Ph layers. Thus, it is very important to know how the APS sealer reacts with the p(AA) polymers chemisorbed to the Zn·Ph. To obtain this information, we created a resemblant reaction model that would yield

interaction products which were detectable using specular reflectance FT-IR over the frequency range 1800 to 1000 cm^{-1}. The samples were prepared by spin-casting at 4000 rpm the 7 wt% APS solution onto a 3 wt% p(AA)-coated aluminum mirror, followed by heating them in an oven at 150°C for 10 min to form the solid-transparent APS film over the p(AA) film. Also, the bulk APS and p(AA) films deposited onto the aluminum mirrors were used as the reference samples. The spectrum of polymeric APS reference film (not shown) had the absorption bands at 1650 and 1600 cm^{-1}, belonging to the CH_2 groups, at 1200 and 1140 cm^{-1}, corresponding to the Si-methoxide compounds [14], and at 1030 cm^{-1} which can be ascribed to the siloxane groups, Si-O-Si [15,16]. The formation of Si-O-Si linkage strongly verified that the transformation of monomeric APS into the polymeric APS occurred during the thermal treatment of films at 150°C. The spectrum of bulk p(AA) indicates the presence of a strong band near 1710 cm^{-1} which can be assigned to the C=O in the pendent carboxyl and the main chain CH_2 of saturated methylene at 1440 cm^{-1}. By comparison with these reference samples, the differences in spectral feature of the p(AA) film coated with the APS were as follows: (1) the disappearance of the peak at 1710 cm^{-1}, (2) the emergence of a new band at 1550 cm^{-1}, and (3) the decrease in peak intensity of the NH_2 band at 1600 cm^{-1}. Regarding the aspect (2), a possible assignment of new band is likely associated with the formation of amide groups, -CONH-, [17,18]. If this assignment is correct, the results strongly demonstrated that when the APS was attached to the p(AA), the NH_2 groups in APS favorably reacted with the carboxyl in p(AA) to form the amide bonds. Thus, it is conceivable that the formation of interfacial amide bonds acts to link strongly p(AA) to the APS films. The hypothetical interaction mechanisms at interfaces between the p(AA)-modified Zn·Ph layer and the polymeric APS sealer are illustrated below:

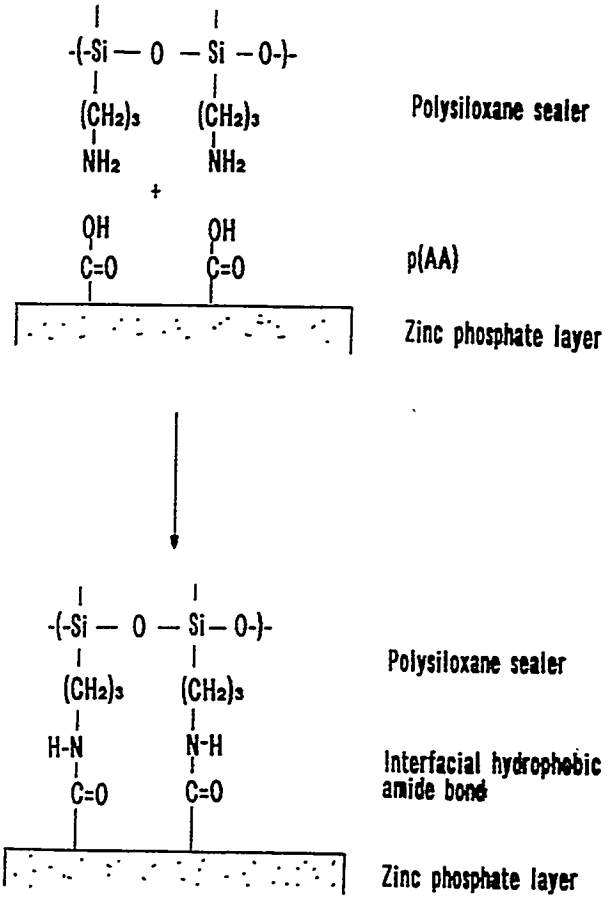

Figure 7 depicts typical polarization curves log current versus potential for the uncoated EGS, and Zn·Ph-and p(AA)-Zn·Ph-coated EGS panels. The shape of the curves presents the transition from cathodic polarization at the onset of the most negative potential to the anodic polarization curves at the end of lower negative potential. The potential axis at the transition point from cathodic to anodic curves is normalized as the corrosion potential, E_{corr}. When compared with those for the uncoated EGS, the striking characteristics of the cathodic curves for the coated EGS specimens are as follows: (1) a decreased current in the vicinity of E_{corr}, and (2) a lower short-term steady-state current value in the potential region between -1.2 and -1.0 V. As a result, it appears that the ability of zinc layers in the EGS to inhibit the cathodic reaction in terms of the oxygen reduction reaction, $H_2O + 1/2O_2 + 2e^- \rightarrow 2OH^-$, of the underlying steel was further enhanced by the p(AA)-modified and unmodified Zn·Ph coatings. Further inhibition of the cathodic reaction by the Zn·Ph coatings not only contributed

significantly to reducing the rate of corrosion of the steel, but also extended lifetime of the zinc layers acting as the corrosion barrier. The polarization curves for the APS-sealed EGS, Zn·Ph/EGS, and p(AA)-Zn·Ph/EGS panels are shown in Figure 8. The thickness of the polymeric APS films deposited to the Zn·Ph-coated and uncoated EGS surfaces was determined using a surface profile measuring system. Their thicknesses ranged from 0.2 to 0.7 μm. A comparison of the cathodic polarization areas from the APS-sealed EGS and unsealed EGS (Fig.7) indicates two noteworthy features: (1) the short-term steady-state current value for the sealed EGS panels is a order of magnitude lower than that of the unsealed one at the potential near -1.0 V; and (2) the APS sealer leads to a shift in corrosion potential to a more positive site and a considerably decreased current in the vicinity of E_{corr}. Regarding the result (1), the lower current for the sealed EGS compared with that of the unsealed one is attributed to a low hydrogen evolution as well as a less active surface of the underlying steel, suggesting that the oxygen reduction reaction is suppressed by the APS sealer. For the second observation, applying the APS sealer to the EGS conspicuously enhanced its resistance to corrosion. When this sealer was applied to the Zn·Ph-coated EGS panels, the curve showed a better corrosion protection than that of the panels in which the APS was directly applied to the EGS; namely, the current in the potential region between -0.9 to -1.0 V became somewhat lower. In contrast, a dramatic improvement in protection by the sealer can be seen from the curve of APS/p(AA)-Zn·Ph/EGS systems, indicating a considerable shift in current to a lower value in the potential range -0.75 to -0.85 V, as well as a large reduction in E_{corr} to a less negative potential. Thus, we believe that the formation of interfacial amide bonds by the interaction between APS and p(AA) significantly contributes to protecting steel from the corrosion, suggesting that the APS has a high potential for use as sealer of the p(AA)-modified Zn·Ph coatings.

Based upon these polarization curves, we attempted to determine the absolute corrosion rates of steel, expressed in the conventional engineering units of milli-inches per year (mpy). The equation (1) proposed by Sterm and Gery [19], was used in the first step:

$$I_{corr} = \beta_a \cdot \beta_c / 2.303 (\beta_a + \beta_c) R_p \text{ ---------- (1)}$$

where I_{corr} is the corrosion current density in A, β_a and β_c having the units of volts/decade of current refer to the anodic and cathodic Tafel slopes, respectively, which were obtained from the log I vs E plots encompassing both

anodic and cathodic regions, and R_p is the polarization resistance which was determined from the corrosion potential, E_{corr}. When I_{corr} was computed through the equation (1), the corrosion rate (mpy) can be obtained from the following expression:

$$\text{Corrosion rate} = 0.13\ I_{corr}\ (EW) / d \text{ ----------(2)}$$

where EW is the equivalent weight of the corroding species in g, and d is the density of the corroding species in g/cm^3.

Table 1 gives the I_{corr} and corrosion rate obtained from this Tafel calculation for various coating panels. The corrosion rate of underlying steel for the uncoated EGS was 1.449 mpy, corresponding to I_{corr} of 3.17×10^{-6} A. This rate was reduced to 0.505 mpy by depositing Zn·Ph onto the EGS surfaces. Incorporating the p(AA) into the Zn·Ph layers has allowed a further reduction to 0.467 mpy. A significant decrease in corrosion rate can be seen from the APS-sealed panels, especially in the APS/p(AA)-Zn·Ph coating system. The rate of 0.022 mpy for this coating system was approximately two orders of magnitude less than that of the uncoated EGS.

In support, all the test panels were exposed in a 5 % salt fog chamber at 35°C to determine the extension of useful lifetime of the coatings that protect the zinc layer in EGS against white rusting. The results from these test panels are shown in Table 2. The consequent data strongly supported the information obtained from the electrochemical polarization experiment; the most promising coating system for mitigating white rust of the zinc layers was the APS-sealed p(AA)-Zn·Ph, conferring a salt-spray resistance for 750 hrs.

3.3 Electrically Deposited Primer Coatings

One important consideration for the sealed Zn·Ph coating systems is to investigate whether the sealer's layers existing at the outermost surface sites of Zn·Ph layers have a proper affinity for the polyurethane-modified epoxy primer coatings (POWERCRON 648). To gain this information, we electrically deposited the primer coatings onto the APS-sealed and unsealed Zn·Ph layers, and then examined the ability of primer coatings to further improve the protection of EGS against corrosion by AC electrochemical impedance spectroscopy (EIS) and the 5 % salt-spray tests according to ASTM D 1654-79a. The thickness of primer coatings ranged from 1 to 2 mil. A schematic representation of the entire coating system developed in this program is illustrated below.

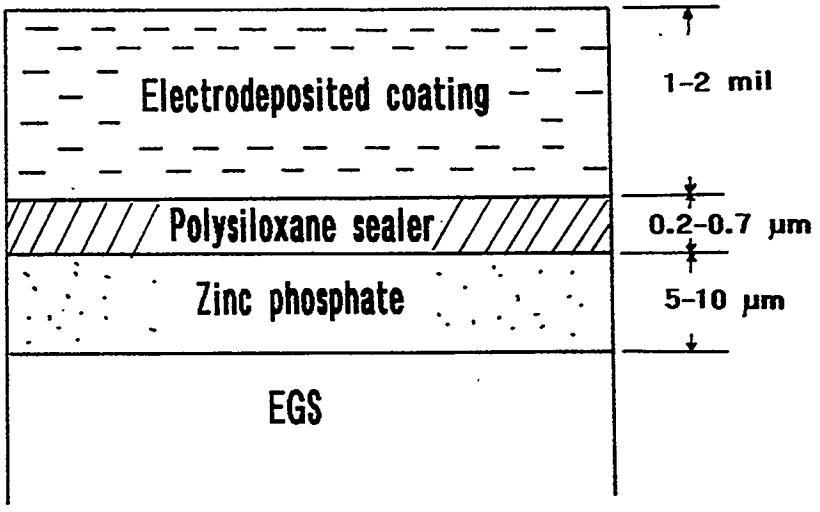

Six different coating systems, electrically deposited primer (EDP), EDP/Zn·Ph, EDP/p(AA)-Zn·Ph, EDP/APS, EDP/APS/Zn·Ph, and EDP/APS/p(AA)-Zn·Ph, were prepared for this examination.

In the EIS tests, the curves (not shown) for all the coated EGS panels depicted the Bode-plot features [the absolute value of impedance $|Z|$ (ohm-cm^2) vs. frequency (Hz)]. Our particular attention in the overall impedance curves was given to the impedance value of the element $|Z|$, which can be determined from the plateau in the Bode plot occurring at sufficiently low frequencies. We adapted the $|Z|$ value at a frequency at 1.5 Hz to compare the magnitudes of ionic conductivity generated by the 0.5 N NaCl electrolyte passing through the coating layers; namely, a high value of $|Z|$ reflects a low degree of penetration of electrolyte into the coating films. Figure 9 gives the changes in $|Z|$ value for these coating panels after for up to 7 days to 0.5 N NaCl solution at 25°C. The

value of |Z| for all coatings tends to decrease slowly with an elapsed exposure time. Thus, the ability of the coatings to reduce the ionic conductivity gradually weakens during exposure, suggesting that a long-term exposure leads to the uptake of more electrolyte by the coatings. The lowest value of |Z| for the EDP-coated EGS panels may be associated with a poor adherence of EDP to the EGS surfaces, thereby resulting in a deficient protective performance. By comparison, the EDP/APS/p(AA)-Zn·Ph and EDP/APS/Zn·Ph coating systems showed an ionically inert behavior, corresponding to $|Z| > 10^7$ ohm-cm^2. Nevertheless, the effectiveness of these coatings in ensuring a low degree of penetration of electrolyte was in the following order; EDP/APS/p(AA)-Zn·Ph > EDP/APS/Zn·Ph > EDP/APS > EDP/p(AA)-Zn·Ph > EDP/Zn·Ph > EDP. Assuming that the factor contributing to the enhancement of protection is due to the chemical attraction of EDP to the substrates, the chemical reaction between the EDP and APS may yield the bond structure which links EDP to APS layers. Although there is no evidence for the chemical reaction mechanisms, we believe that such interfacial interactions play an important role in protecting EGS panels from the corrosion.

This information was correlated directly with the states of primer-coated panels after salt-spray tests for 1080 hours. A scribe of the panels down to bare metal was meant to simulate mechanical damage of the primer coating, where failure can begin easily. The delamination of coating film from the substrate corresponds to the loss of adhesion of the film at the defect, and is the major reason for the scribe. Two major failures were generally looked for in evaluating the results from salt-sprayed specimens: 1) the degree of blistering of the film in inscribed areas, and 2) the delamination of film surrounding the blemish from substrates. The results from these test panels are shown in Table 3. The EDP-coated EGS panels without the APS sealer and Zn·Ph coating showed the failures of the protective coatings after exposure to the salt fog for only 360 hours. The two features considered as failures were 1) the average loss of 10 mm coating films from a scribe mark, and 2) the occupation of ≈ 80 % of the inscribed areas by blisters. By comparison, the deposition of p(AA)-modified Zn·Ph and unmodified Zn·Ph coatings onto the EGS contributed remarkably to protecting EGS from salt-induced corrosion during an exposure of 1080 hours. A further improvement in protection was observed when both the EGS substrate and Zn·Ph coating were treated with the APS. Although some peeling and blistering were observed surrounding the blemished film and in the unblemished areas, the EDP coating

overlaid on the APS/p(AA)-Zn·Ph layers displayed the best protective performance, compared with any other coating systems. The EDP/APS/Zn·Ph coating system gave the second best protective performance. This finding was similar to the data on the EIS: the most effective coating system for protecting EGS against corrosion was identified to be the EDP/APS/p(AA)-Zn·Ph.

3.4 Industrial-Scale Demonstration Tests

To demonstrate the reproducibility of this coating technology on mini-sized automobile door panels (25 cm x 25 cm x 5 cm in size) made from EGS, a full-scale feasibility test was carried out in collaboration with the Palnut Company, New Jersey, on December 3, 1996 (Fig. 10).

As described in the Experimental section, the optimized Zn·Ph coating process technology, except for the EDP coating, involved the cleaning, coating, rinsing, sealing, and drying (Fig. 11). The four separate solution tanks with a 1514 L (400 Gal.) were used in a whole process, excepting for the drying. First, the fifteen mini-sized EGS door panels on hangers were immersed in a pickling solution for 1 min at 25°C to remove any surface contaminants (Fig. 12). Second, the cleaned panels were soaked into the p(AA)-modified zinc phosphate make-up solution for 1 min at 80°C (Fig. 13), withdrawn slowly (Fig. 14), and rinsed with water. Third, the water-rinsed panels were dipped for few seconds into the APS sealant (Fig. 15), and finally, the APS-wetted Zn·Ph panels were dried in an oven for 30 min at 150°C to convert the precursor solution into the polymeric APS sealer (Fig. 16). Then, a visual observation was made to ensure that uniform, dense, continuous Zn·Ph layers completely were covered over the EGS surfaces (Fig. 17). The total preparation time of coatings was ≈ 35 min. To ensure that this coating process was reproducible, the procedure was repeated ten times; all 150 mini-sized door panels were successfully coated with Zn·Ph. Half of them was sent to ACT Laboratories, INC. to make electrodeposited primer coatings. After all the primed panels are returned to us, environmental testing of these panels will commence at Tacom, BNL, and other Army engineering laboratories.

4. Conclusions

We modified the surface of electrogalvanized steels (EGS) to inhibit corrosion of Zn layers and to improve their sealer-adhesion properties by

immersing EGS panels into environmentally acceptable zinc phosphating solutions consisting of $Zn_3(PO_4)_2 \cdot 2H_2O$, H_3PO_4, poly(acrylic acid)[p(AA)], $Mn(NO_3)_2 \cdot 6H_2O$ and water at 80°C. The electrochemical reaction between Mn dissociated from $Mn(NO_3)_2 \cdot 6H_2O$ and Zn in the acid media created short-circuited cells by the flow of electrons from Zn acting as the anode to Mn as the cathode. Such a cathodic activity increasingly promotes the anodic dissolution of Zn, $Zn \rightarrow Zn^{2+} + 2e^-$, and is reflected by a brisker evolution of hydrogen from the Mn. Considering the precipitation of crystalline zinc phosphate tetrahydrate (hopeite) on the EGS surface, a high degree of ejection of Zn ions contributed significantly to the rapid growth of hopeite crystals deposited on EGS. Uniform hopeite layers completely converting over the EGS surfaces were observed on the specimens prepared by immersion for only 5 sec, thereby conferring good protection layers against corrosion. Thus, it is apparent that the service life of Zn layers as protective barriers for underlying steels could be extended. Hexavalent Cr acids known to be environmental hazards are commonly used as a sealant for the Zn·Ph layers because they improve the ability of Zn·Ph to protect the metal from corrosion. Hence, our attention was paid to find the replacing materials for the Cr acids. We succeeded in developing an environmentally acceptable water-based 3-aminopropyltrimethoxysilane (APS) sealant, which is converted into a polymeric APS sealer at 150°C. When the APS was applied to the surfaces of p(AA)-modified Zn·Ph layers, the carboxyl groups in the p(AA) existing at the outermost surface sites of Zn·Ph layers chemically reacted with the amino groups in the APS sealer to form amide bonds at interfaces between Zn·Ph and APS layers. This interfacial amid bond which linked the Zn·Ph to APS significantly contributed to protecting EGS from the white rust corrosion, which represents deterioration of the zinc layer in EGS, suggesting that the APS has a high potential as a replacing sealant. In addition, the APS sealer had a strong chemical affinity for the polyurethane-modified epoxy primer coating induced by the electrodeposition technology. Such affinity at the critical boundary zones not only led to the coverage of a smooth, continuous primer film over the Zn·Ph layers, but also acted to confer a great protection of EGS against corrosion.

We conducted a scale-up test to demonstrate the reproducibility of this coating technology on mini-sized automobile door panels made from EGS in collaboration with the Palnut Company in New Jersey. Fifteen mini door panels were successively emersed in four separate solution tanks (holding 400 gal.),

involving a cleaning, coating, rinsing, and sealing; the total preparation time was ≈ 35 min. This process was repeated ten times and all 150 panels were successfully coated with APS-sealed Zn·Ph, thereby establishing the potential for industrial-scale feasibility of this coating technology.

5. Recommendations

The following five recommendations from the integration of our work performed in FY 96 as Phase II research, are described below:

1. The optimum formulation for an environmentally benign zinc phosphating solution suitable for electogalvanized steels (EGS) was 5 wt% $Zn_3(PO_4)_2 \cdot 2H_2O$ powder, 10 wt% (85 % H_3PO_4), 1.0 wt% $Mn(NO_3)_2 \cdot 6H_2O$, and 84 wt% water, in conjunction with poly(acrylic acid) [p(AA), M.W. 60,000] additive of 3.0 wt% by total weight of basic zinc phosphating solution.

2. The water-based 3-aminopropyltrimethoxysilane (APS) sealant consisting of a 7 wt% APS, 3 wt% methylalcohol, 0.7 wt% hydrochloric acid, and 89.3 wt% water, can be used to replace the conventional hexavalent Cr acid sealant. The conversion of APS precursor solution into the polymeric APS sealer was carried out by heating it for 30 min at 150°C.

3. Using the process technology developed in this work, the p(AA)-modified zinc phosphate (Zn·Ph) conversion coatings with a APS sealer were prepared in according with the following sequence: 1) pickling the EGS panels in a 2 wt% H_3PO_4-1 wt% H_2SO_4-97 wt% water solution for 1 min at 25°C, 2) immersing the surfaces-cleaned EGS panels for 1 min into the p(AA)-dissolved zinc phosphate solution at 80°C, 3) rinsing the Zn·Ph-coated EGS surfaces with water, 4) dipping the water-rinsed Zn·Ph coating panels for few seconds into a 7 wt% APS sealing agent at 25°C, and 5) drying the APS-wetted Zn·Ph coating panels for 30 min in an oven at 150°C.

4. Although this coating technology is feasible for depositing corrosion-protective Zn·Ph coatings to the EGS on the industrial scale, we will need a long-term exposure in a corrosive environment to ensure that they afford an adequate protection of EGS against corrosion.

5. This coating system was responsible for improving the corrosion resistance of auto-motive body panels made of EGS by delaying the onset of "white rust", which represents deterioration of the zinc layer in EGS. However, the assessment of the potential application of this coating system to the bare steel vehicles was unfinished. Thus, again, a full-scale demonstration test will be required for verifying the industrial feasibility of the coating technology that inhibits the onset of "red rust" of various discrete parts, such as fasteners and brackets.

6. Acknowledgments

The authors are grateful to Dr. Robert R. Reeber, U.S. Army Research Office (ARO), for his invaluable suggestions; and to Dr. Joseph Lucas, PPG Industries, Inc., for his assistance to prepare electrodeposited topcoatings on the Zn·Ph surfaces. Discussions with Mr. Philip H. Austin, the Palnut Company, is also appreciated.

References

1. C.I. Handsy, T. Sugama, and N. Carciello, Advanced Polyelectrolyte-Modified Zinc Phosphate Coatings, Phase I, SERDP Final Report, 1995.
2. R. Sard, Plat. and Surf. Fin. 74 (1987) 30.
3. E. Breval, and M. Rachlity, J. Mater. Sci. 28 (1988) 1835.
4. T. Sugama, and R. Broyer, Surf. Coatings Tech. 50 (1992) 89.
5. M. Pelavin, D.N. Hendrickson, J.M. Hollander, and W.L. Jolly, J. Phys. Chem. 74 (1970) 1116.
6. G. Schoen, J. Electron Spectrosc. Relat. Phenom. 2 (1973) 75.
7. J.E. DeVries, J.W. Holubka, and R.A. Dickie, J. Adhesion Sci. Tech, 3
8. T. Sugama, L.E. Kukacka, N. Carciello, and J.B. Warren, J. Coatings Tech. 61 (1989) 43.
9. T. Sugama, L.E. Kukacka, C.R. Clayton, and H.C. Hua, J. Adhesion Sci. Tech. 1 (1987) 265.
10. D. Briggs, and M.P. Seach. "Practical Surface Analysis by Auger and X-Ray Photoelectron Spectroscopy", John Wiley, New York, (1985) p 385.
11. P.S. Ho, P.O. Hahn, J.W. Bartha, G.W. Rubloff, F.K. LeGoues, and B.D. Silverman, J. Vac. Sci. Tech. 3 (1985) 739.
12. F.S. Ohuchi, and S.C. Freilich, J. Vac. Sci. Tech. 4 (1986) 1039.
13. H. Leidheiser, Jr., and I. Suzuki, J. Electrochem. Soc. 128 (1981) 241.
14. A.L. Smith, Spectrochim. Acta, 16 (1960) 87.
15. G.J. Su, N.F. Borelli, and A.R. Miller, Phys. Chem. Glasses, 3 (1962) 167.
16. R. Hama, J. Am. Ceram. Soc., 48 (1965) 595.
17. I. Mizushima, T. Shimanouchi, I. Ichishima, T. Miyazawa, I. Nakagawa, and T. Araki, J. Amer. Chem. Soc., 78 (1957) 2038.
18. M.St.C. Flett, Spectrochim Acta, 18 (1962) 1537.
19. M. Sterm, and A.L. Geary, J. Electrochem. Soc., 104 (1957) 56.

Table 1. Tafel Analyses for Polarization Curves of Coated EGS Panels

Coating	E_{corr}(I=0) V	β_a V/decade	β_c V/decade	I_{corr} A	Corrosion rate mpy
Uncoated	-0.8711	0.0669	0.1513	3.17×10^{-6}	1.449
Zn·Ph	-0.9692	0.0472	0.1660	1.11×10^{-6}	0.505
p(AA)-Zn·Ph	-0.9609	0.0668	0.1547	1.03×10^{-6}	0.467
APS	-0.8293	0.0458	0.1312	3.10×10^{-7}	0.142
APS/Zn·Ph	-0.8453	0.0532	0.1227	2.12×10^{-7}	0.097
APS/p(AA)-Zn·Ph	-0.6421	0.1257	0.1634	4.78×10^{-8}	0.022

Table 2. Salt-Spray Resistance of Coated EGS Panels

Coating	Salt-spray resistance, Hr
Uncoated	15
Zn·Ph	190
p(AA)-Zn·Ph	264
APS	340
APS/Zn·Ph	612
APS/p(AA)-Zn·Ph	750

Table 3. Evaluation of EDP-Coated EGS Panels Subjected to 5 % Salt Spray Testing

Coating	Exposure hr	Representative mean creepage from scribe mm	Area of blister formed in inscribed areas %
EDP	360	10.0	≈ 80
EDP/Zn·Ph	1080	8.5	≈ 32
EDP/p(AA)-Zn·Ph	1080	6.5	≈ 28
EDP/APS	1080	3.0	≈ 20
EDP/APS/Zn·Ph	1080	1.8	≈ 13
EDP/APS/p(AA)-Zn·Ph	1080	1.2	≈ 5

LEGENDS FOR FIGURES

Figure 1. SEM image of p(AA)-modified zinc phosphate deposited rapidly on EGS surfaces after immersion for 1 sec (a), 2 sec (b), 5 sec (c), and 10 sec (d).

Figure 2. XPS P_{2p} and $Zn_{2p3/2}$ regions of Zn·Ph deposited on EGS as a function of immersion time.

Figure 3. C_{1s} region of "as-received" EGS (0S), and 2s and 10s-treated Zn·Ph surfaces.

Figure 4. Changes in the concentration of zinc ions dissolved anodically from galvanized coating after immersion of EGS into H_3PO_4, $Mn(NO_3)_2 \cdot 6H_2O$, and H_3PO_4 + $Mn(NO_3)_2 \cdot 6H_2O$ solution, respectively, at 80°C.

Figure 5. Hypothetical multiple reactions occurring at interfaces between EGS and Mn-incorporated H_3PO_4 electrolyte.

Figure 6. XRD patterns of "as-received" EGS surfaces as control, and Zn·Ph made after immersion for 1, 2, 5, and 10s.

Figure 7. Polarization curves for "as-received" EGS, and p(AA)-modified and unmodified Zn·Ph coating panels.

Figure 8. Polarization curves for the APS-sealed EGS, Zn·Ph, and p(AA)-Zn·Ph panels.

Figure 9. Changes in impedance value for (0) EDP-, (●) EDP/Zn·Ph-, (▲) EDP/p(AA)-Zn·Ph-, (□) EDP/APS-, (△) EDP/APS/Zn·Ph-, and (0) EDP/APS/p(AA)-Zn·Ph-coated EGS panels as a function of exposure time.

Figure 10. Production line of Zn·Ph coatings at Palnut Company.

Figure 11. Process technology for Zn·Ph coatings on EGS.

Figure 12. Anticipating the first pickle bath for the fifteen panels on hanger.

Figure 13. Immersing the fifteen panels into the second bath which is zinc phosphate make-up solution at 80°C.

Figure 14. Removing the panels from zinc phosphate bath after 1 min immersion.

Figure 15. Anticipating the fourth bath which is APS sealing solution for the water-rinsed Zn·Ph panels.

Figure 16. Fifteen panels are drying on a conveyor belt in air oven at 150°C.

Figure 17. After drying, panels are being examined visually.

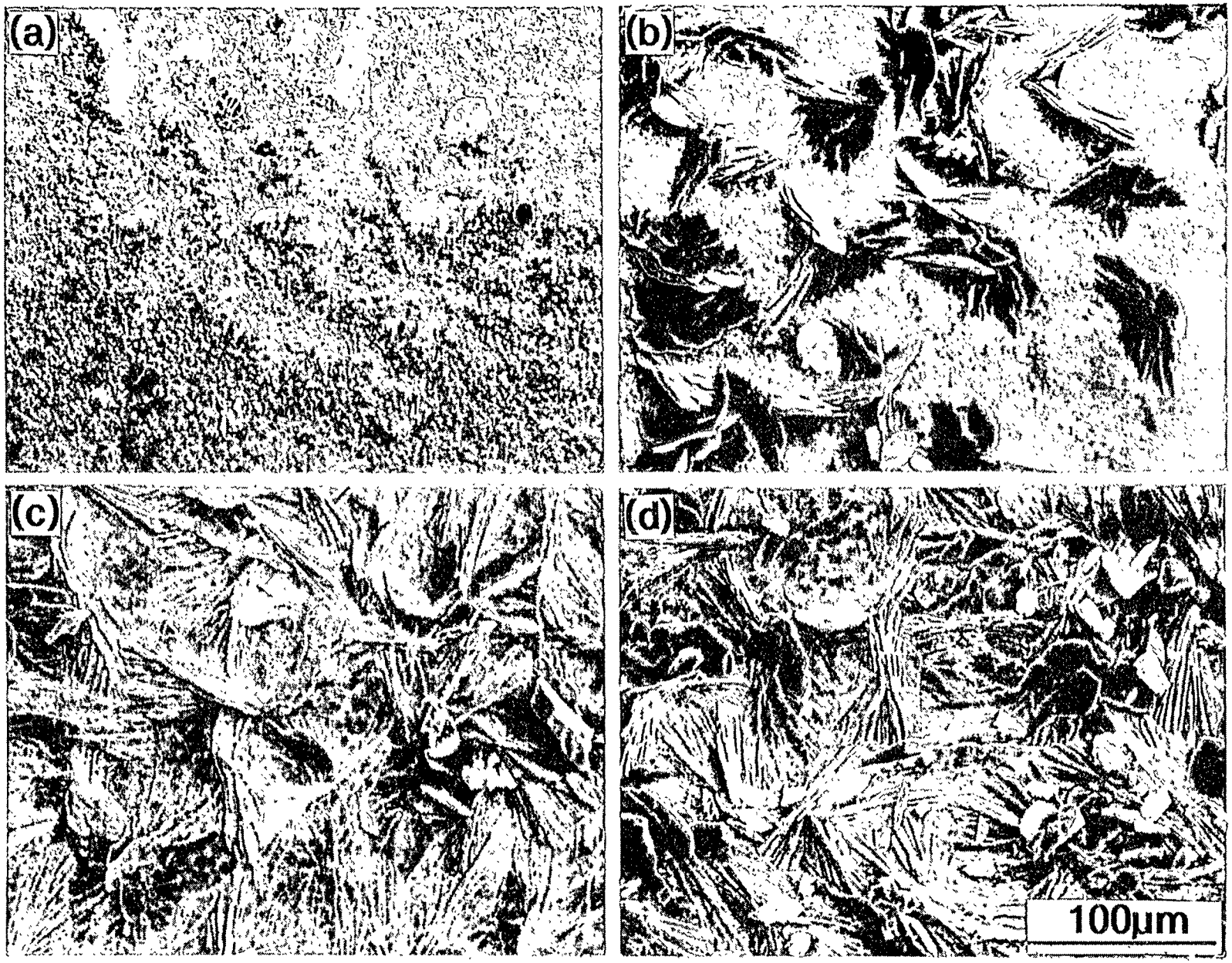

Figure 1. SEM image of p(AA)-modified zinc phosphate deposited rapidly on EGS surfaces after immersion for 1 sec (a), 2 sec (b), 5 sec (c), and 10 sec (d).

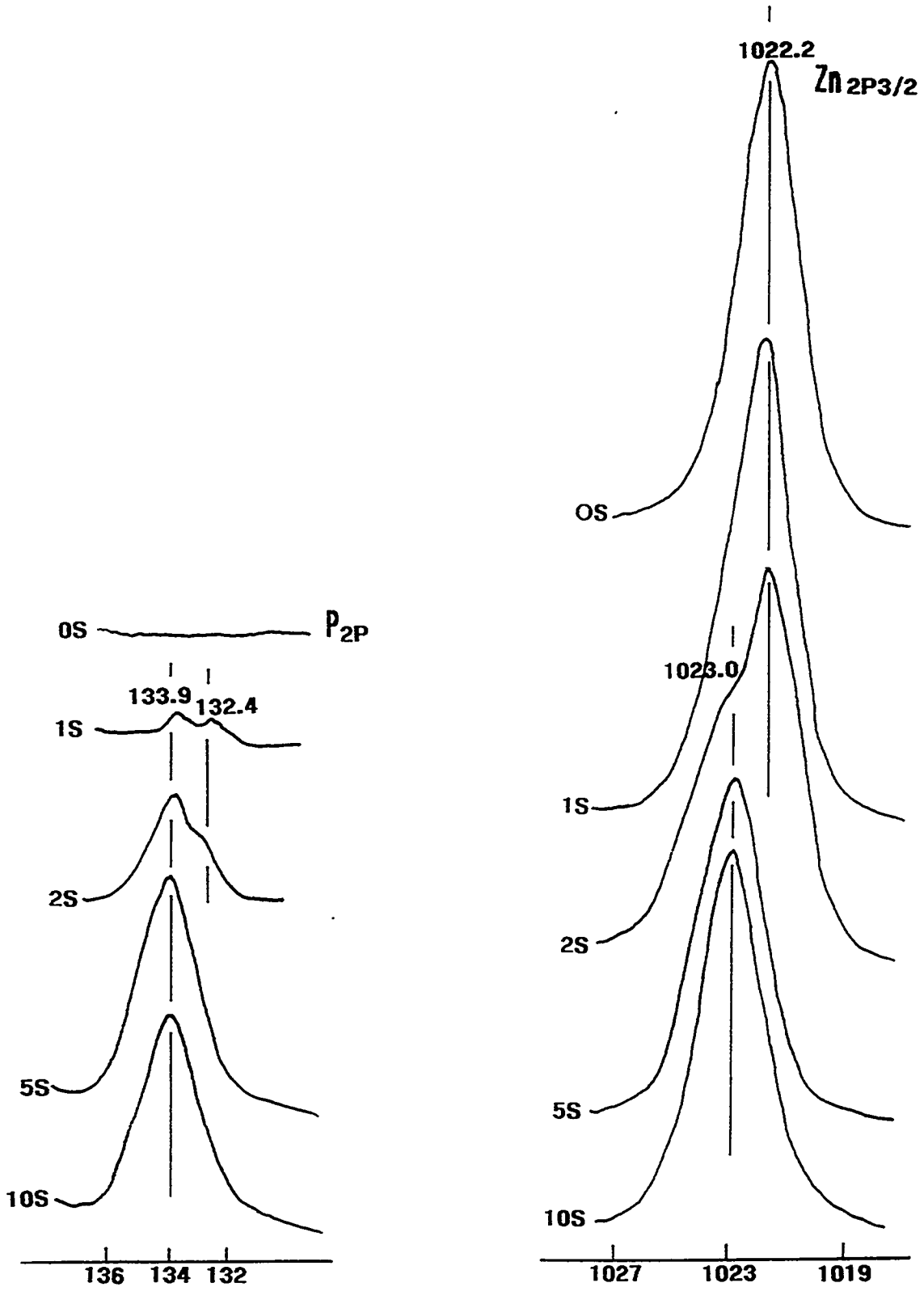

Figure 2. XPS P_{2p} and $Zn_{2p3/2}$ regions of Zn·Ph deposited on EGS as a function of immersion time.

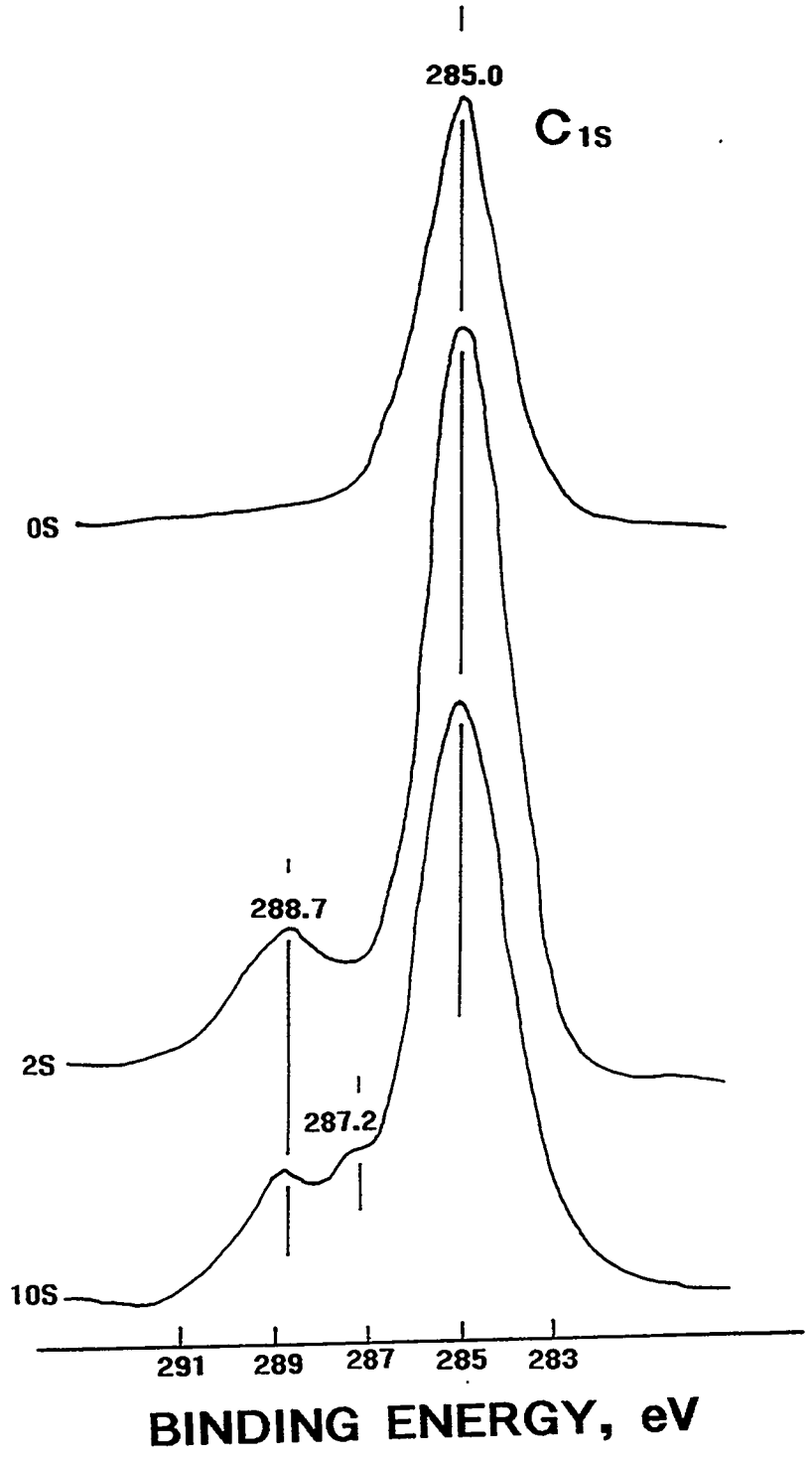

Figure 3. C_{1s} region of "as-received" EGS (0S), and 2s and 10s-treated Zn·Ph surfaces.

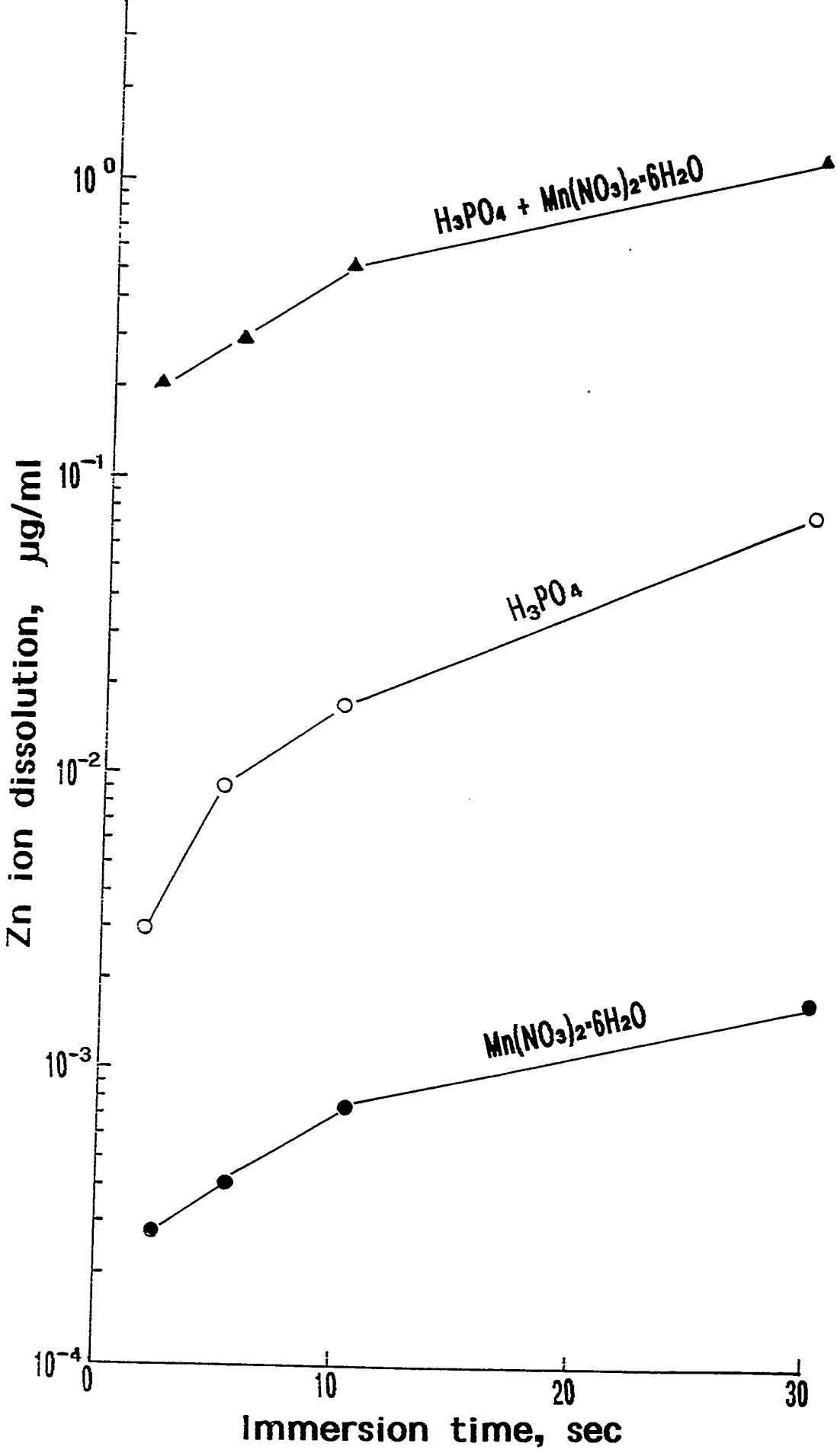

Figure 4. Changes in the concentration of zinc ions dissolved anodically from galvanized coating after immersion of EGS into H_3PO_4, $Mn(NO_3)_2 \cdot 6H_2O$, and $H_3PO_4 + Mn(NO_3)_2 \cdot 6H_2O$ solution, respectively, at 80°C.

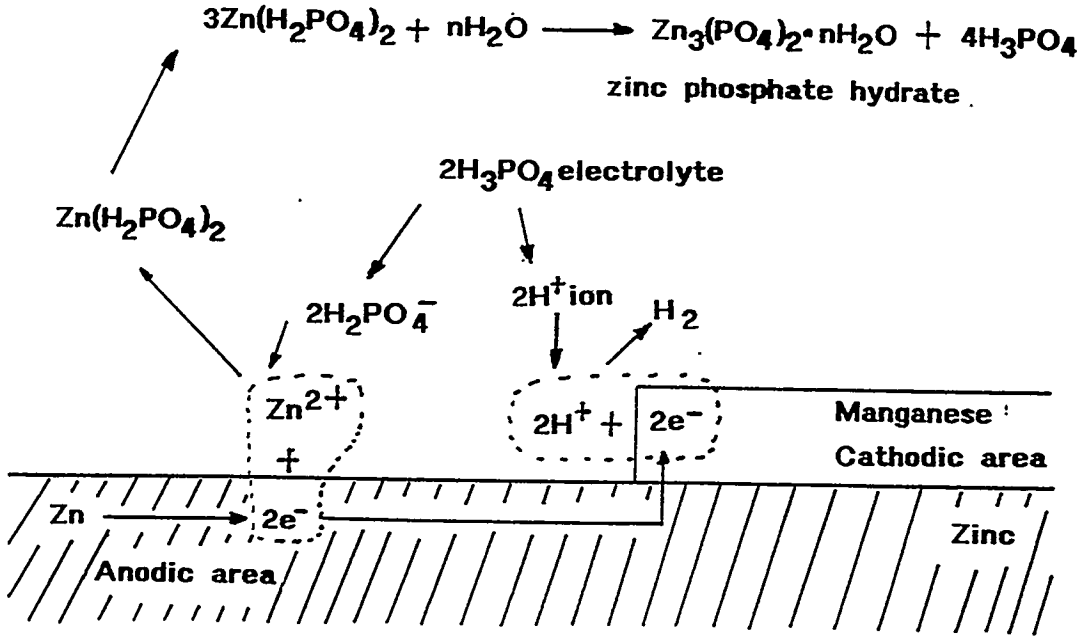

Figure 5. Hypothetical multiple reactions occurring at interfaces between EGS and Mn-incorporated H_3PO_4 electrolyte.

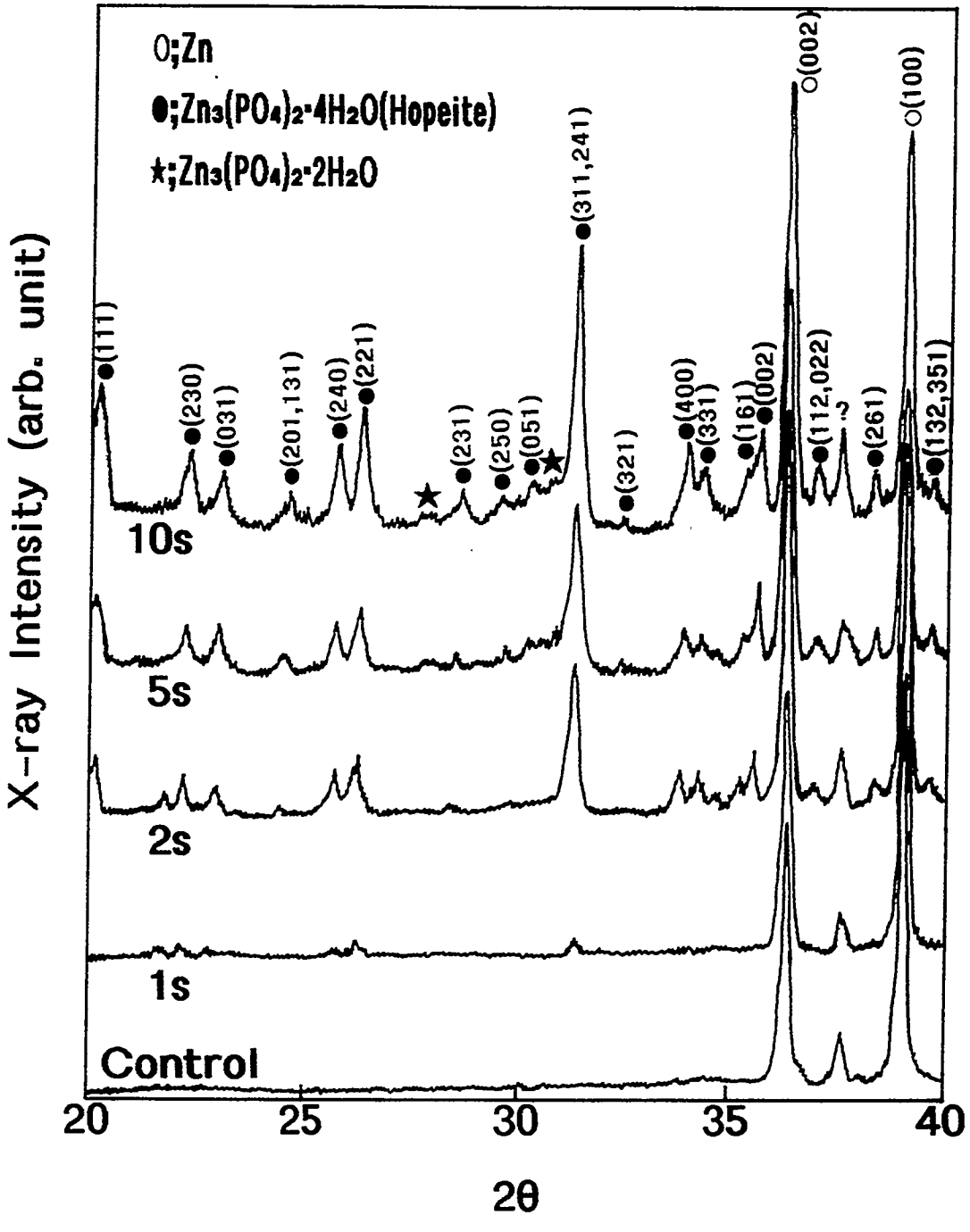

Figure 6. XRD patterns of "as-received" EGS surfaces as control, and Zn·Ph made after immersion for 1, 2, 5, and 10s.

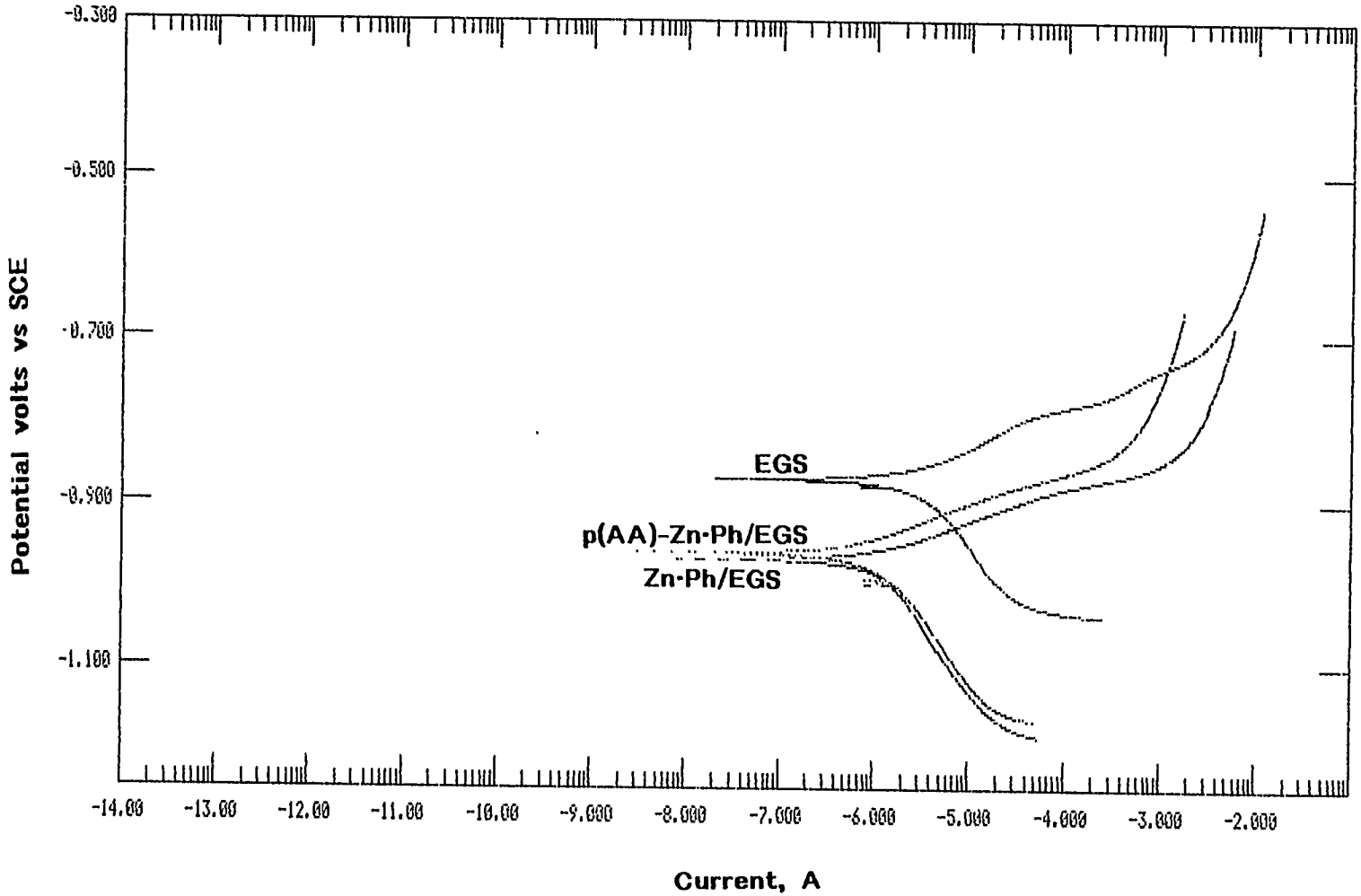

Figure 7. Polarization curves for "as-received" EGS, and p(AA)-modified and unmodified Zn·Ph coating panels.

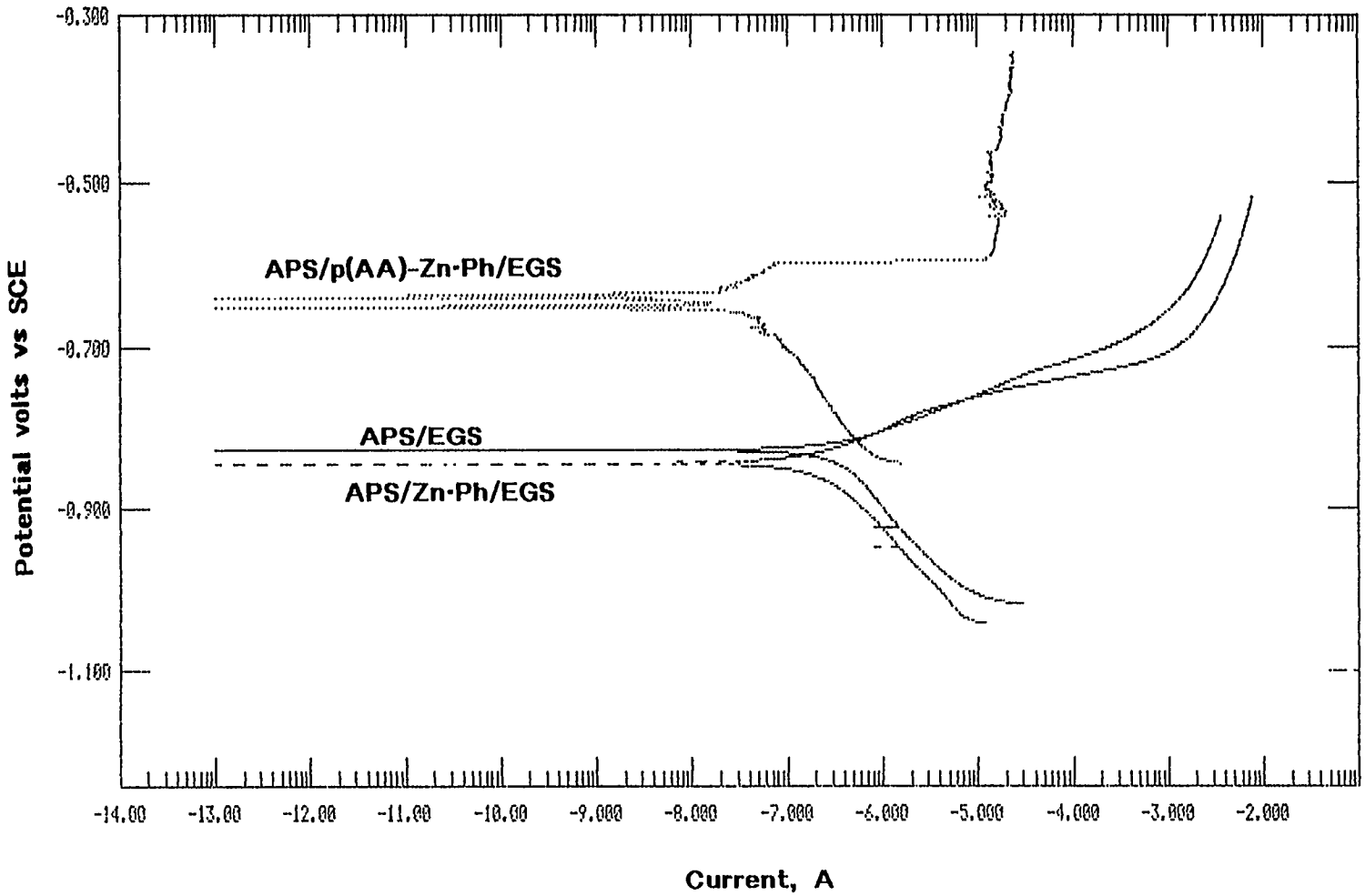

Figure 8. Polarization curves for the APS-sealed EGS, Zn·Ph, and p(AA)-Zn·Ph panels.

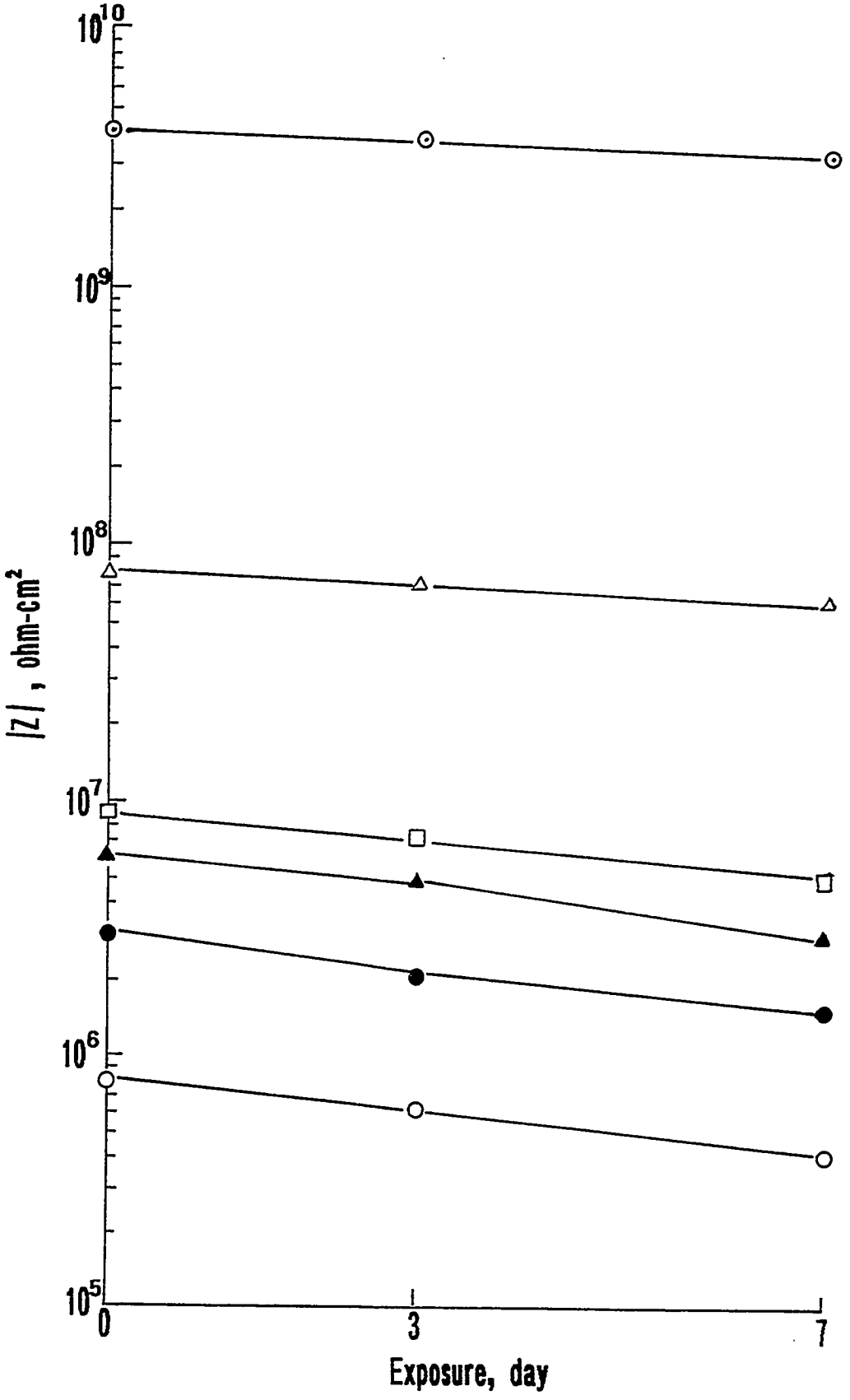

Figure 9. Changes in impedance value for (0) EDP-, (●) EDP/Zn·Ph-, (▲) EDP/p(AA)-Zn·Ph-, (□) EDP/APS-, (△) EDP/APS/Zn·Ph-, and (0) EDP/APS/p(AA)-Zn·Ph-coated EGS panels as a function of exposure time.

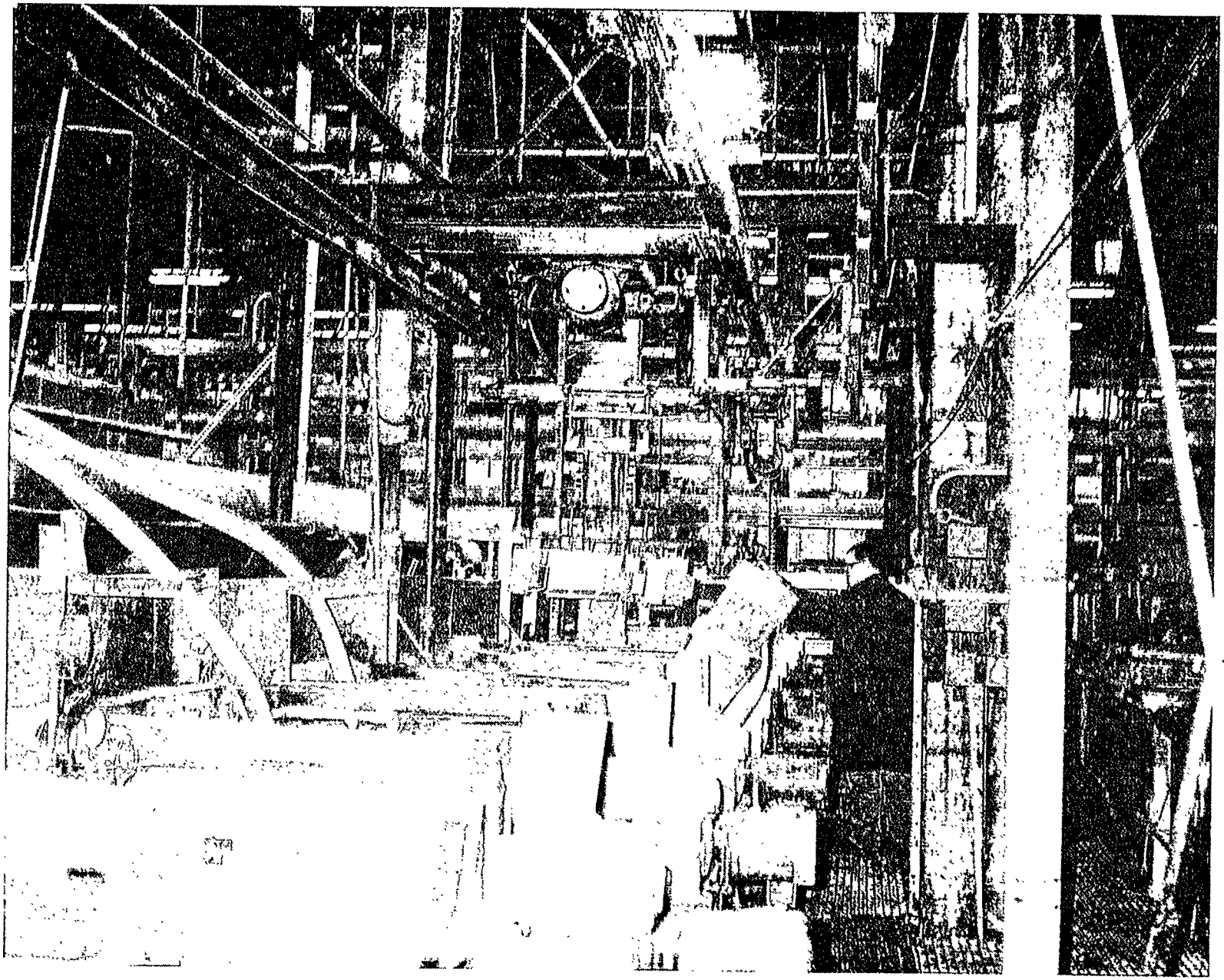

Figure 10. Production line of Zn·Ph coatings at Palnut Company.

1. Pickled (2 wt% H_3PO_4-1 wt% H_2SO_4-97 wt% water) for 1 min at 25°C

2. Immersed in zinc phosphate solution for 1 min at 80°C

3. Rinsed with water

4. Dipped in water-based polysiloxane sealant

5. Oven-dried for 30 min at 150°C

6. Electrodeposited primer coatings

Figure 11. Process technology for Zn·Ph coatings on EGS.

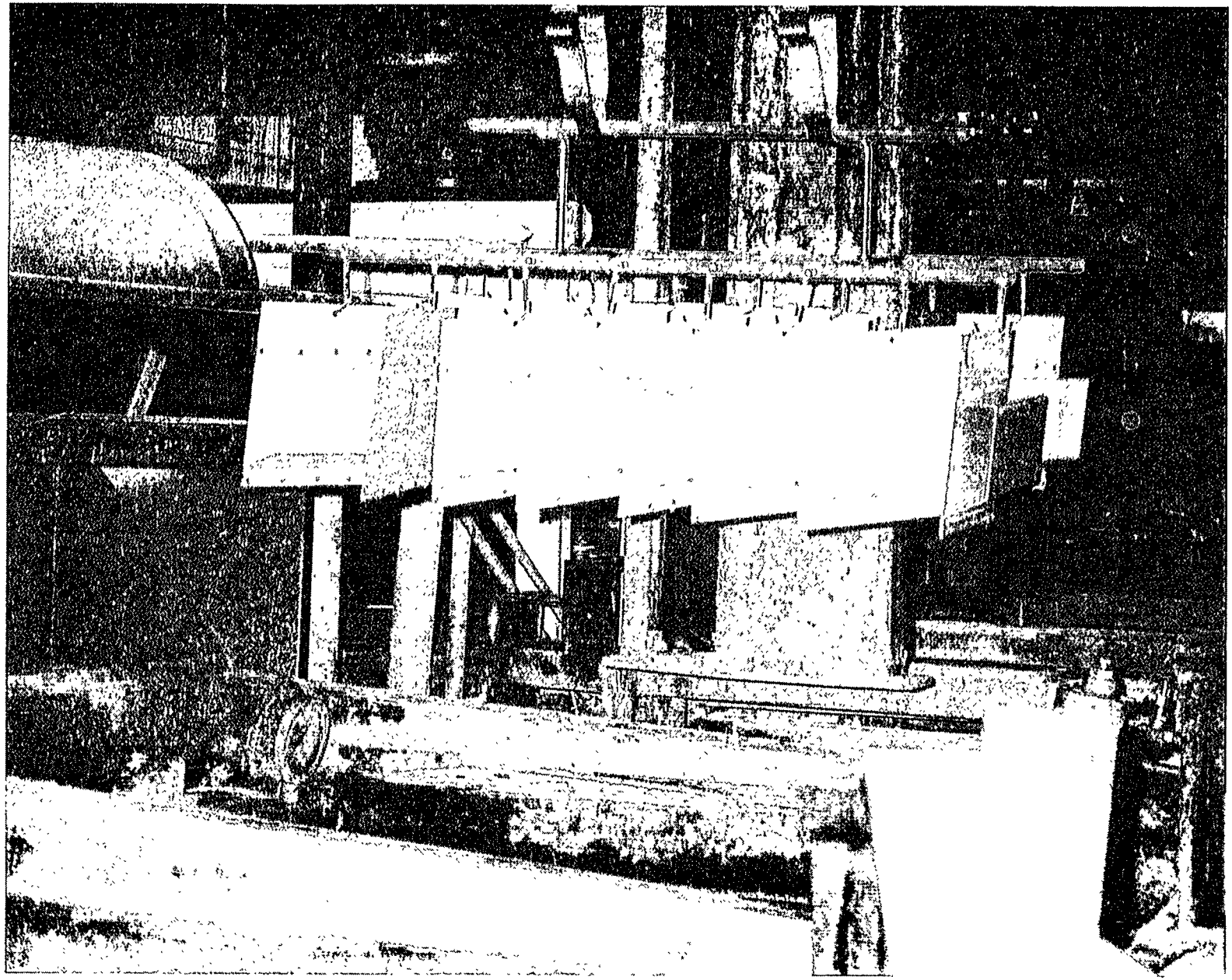

Figure 12. Anticipating the first pickle bath for the fifteen panels on hanger.

Figure 13. Immersing the fifteen panels into the second bath which is zinc phosphate make-up solution at 80°C.

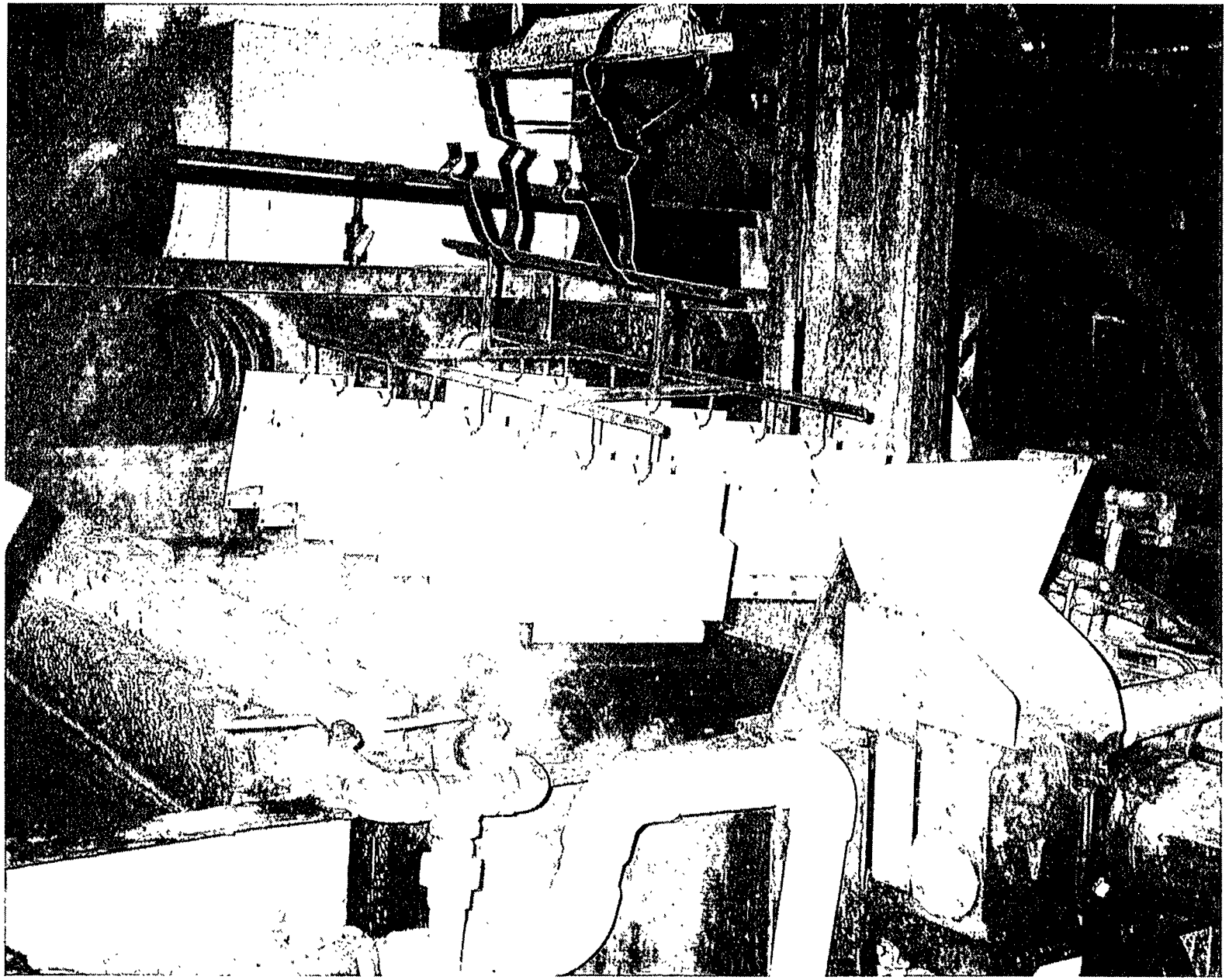

Figure 14. Removing the panels from zinc phosphate bath after 1 min immersion.

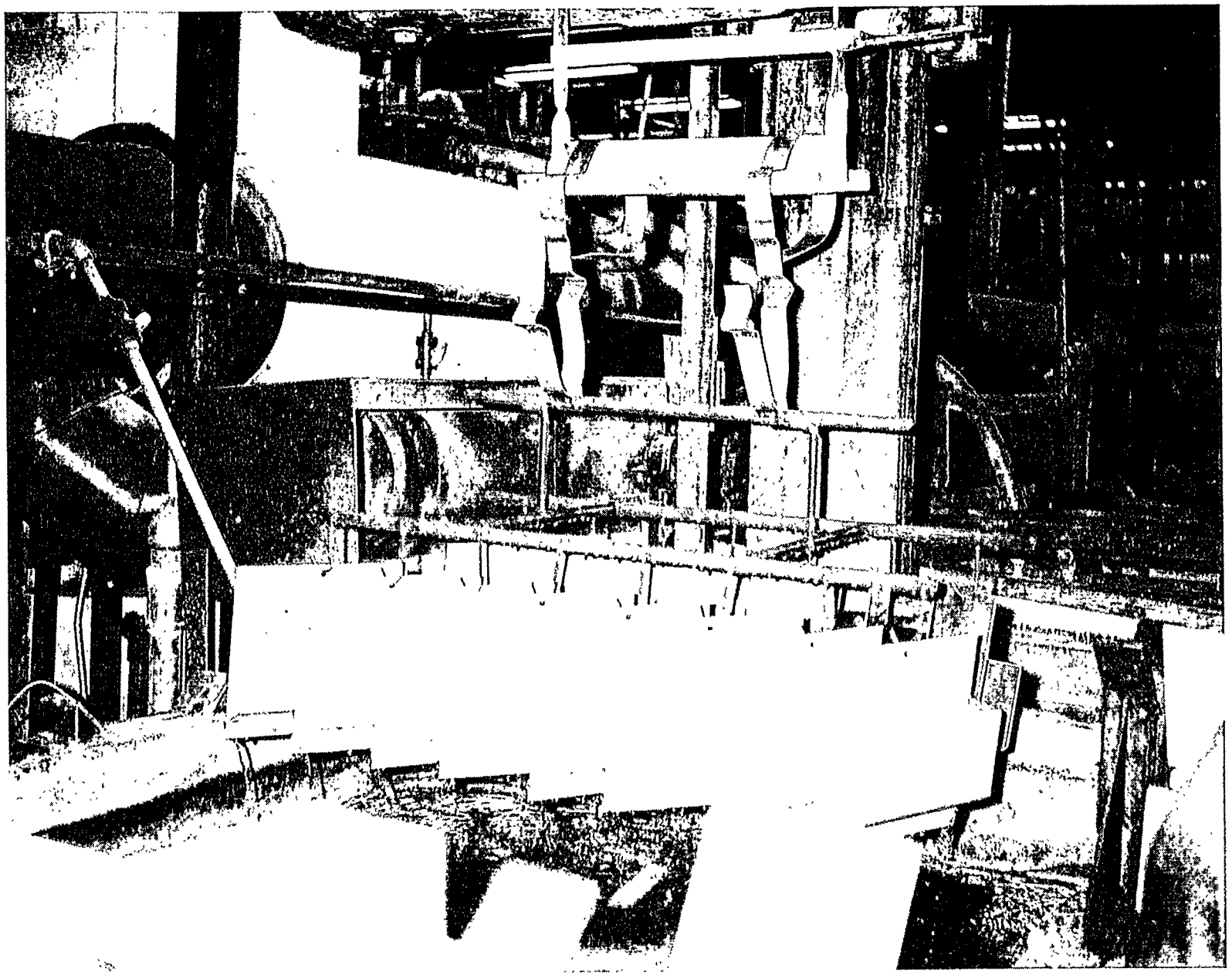

Figure 15. Anticipating the fourth bath which is APS sealing solution for the water-rinsed Zn·Ph panels.

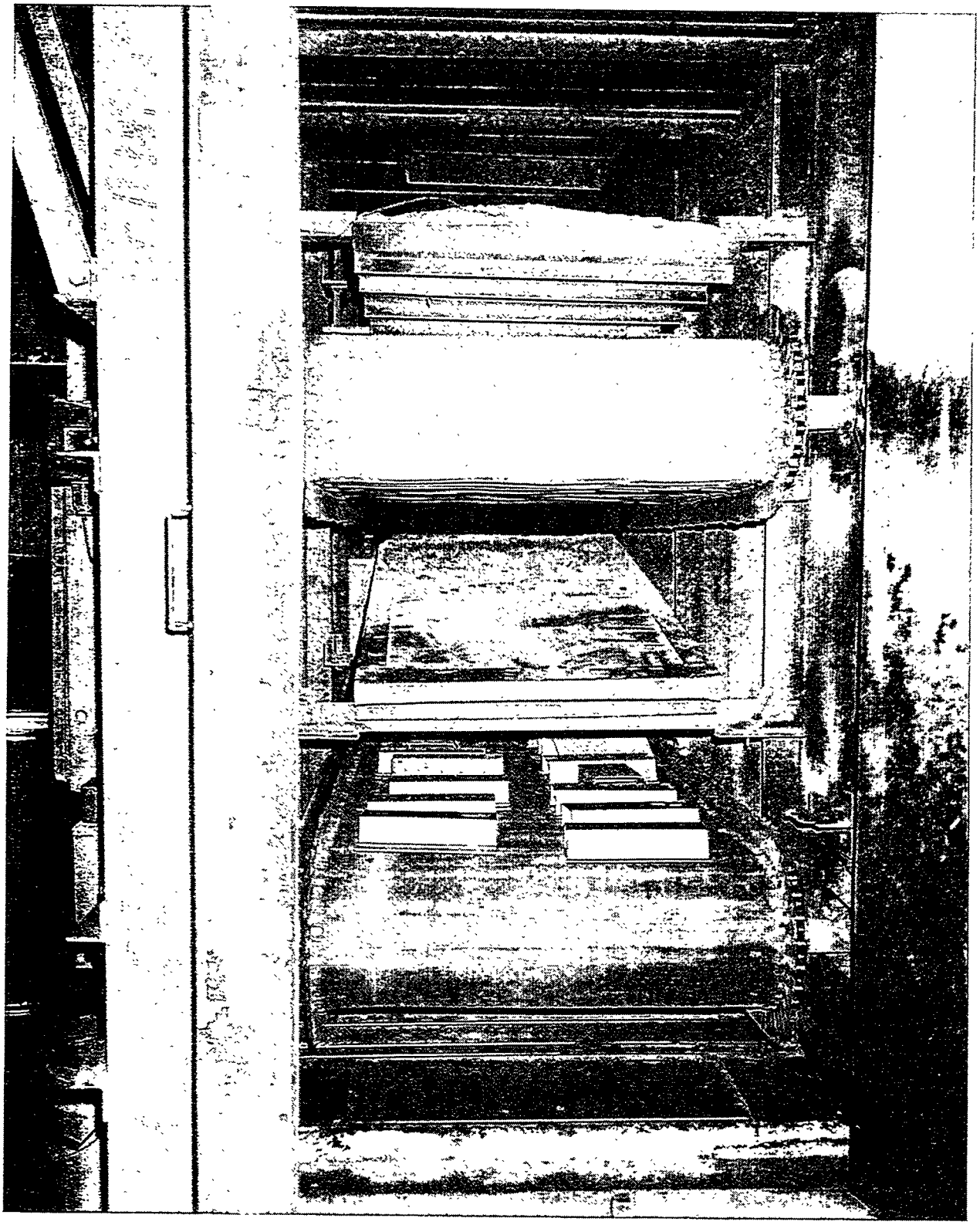

Figure 16. Fifteen panels are drying on a conveyor belt in air oven at 150°C.

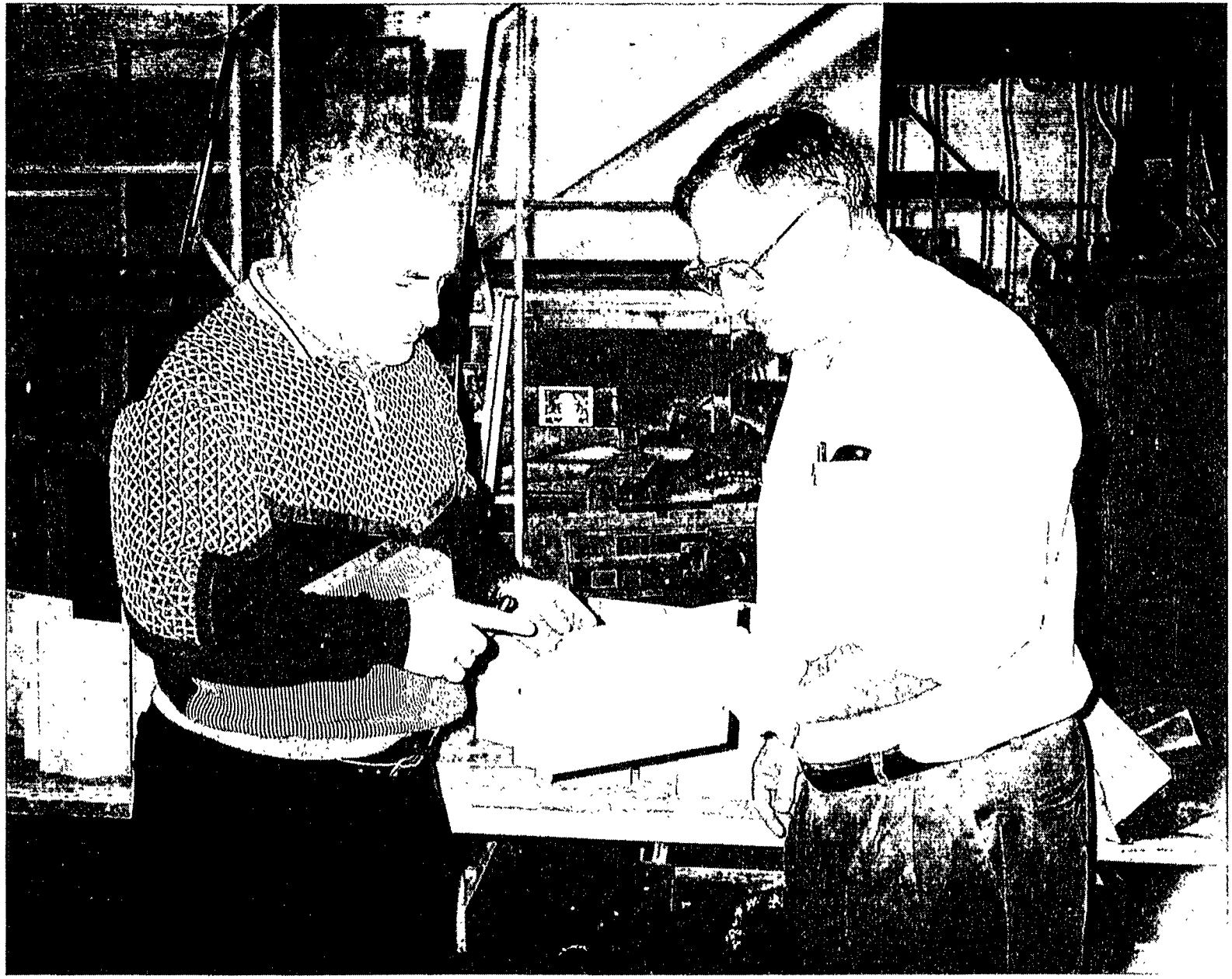

Figure 17. After drying, panels are being examined visually.